Saudi Journal of Ophthalmology (2014) 28, 220—224

Original Article

Three dimensional MRI study: Safety of short versus long needle peribulbar anesthesia☆

Sahar M. ElKhamary, MD[a,b,*]; Waleed Riad, MD, AB, SB, KSUF[c]

Abstract

Background: The standard technique of Peribulbar block is to use 25 g 25 mm needle at the junction between the lateral one third and medial two third of the lower orbital rim in the infero-temporal quadrant of the orbit. Theoretically, insertion of longer needles increases the potential of injury to important structure; however, safety of the shorter needle had never been demonstrated. This study describes the anatomy of the orbital structures with magnetic resonance imaging (MRI) using the three-dimensional constructive interference in steady state (3D CISS) sequence to present a morphological basis for needle entry at 12.5 and 25 mm lengths. Statistical comparisons were performed at the 12.5 versus 25 mm depths. Statistical significance was indicated by $P < 0.05$.

Method: Fifty patients free of orbital pathology with normal axial length were selected for MRI with the 3D CISS sequence. Original axial and multiplanar image reconstruction (MPR) images were selected for image interpretation. Orbital structures were identified at 12.5 and 25 mm depths from the orbital rim to compare significant differences in anatomy between the two imaging planes at the expected needle depth and to assess the size of the globe and the orbit.

Results: The cross sectional area of the extraocular muscles were statistically significantly smaller at the 12.5 mm plane ($P = 0.001$). The area of inferotemporal fat was statistically significantly larger at the 12.5 mm plane ($P = 0.033$). There was no statistical difference in the inferonasal and superonasal fat areas at different depths ($P = 0.34$, $P = 0.35$ respectively). The size of the orbit and globe was significantly larger at 12.5 mm ($P = 0.001$). There was no difference between depths in the presence or absence of neurovascular bundles and supporting structures including the intramuscular septae.

Conclusion: There is a larger structure-free space at a depth of 12.5 mm than at 25 mm. Therefore, the inference is that a needle inserted in the infero-temporal zone to a depth of 12.5 mm is less likely to injure the eyeball or extra-ocular muscles than one advanced to 25 mm.

Keywords: MRI 3D-CISS, Short needle, Peribulbar anesthesia

http://dx.doi.org/10.1016/j.sjopt.2014.03.002

Introduction

Needle length is one important consideration for the safe conduct of an ophthalmic block. Short, 12.5 mm needle injection technique for percutaneous peribulbar anesthesia is an alternative to the standard longer 25 mm needle.[1–5] Previously, Winder et al.[1] and Van den berg coauthors[4] demonstrated that peribulbar blockade with a 15 mm needle combined with digital compression is equally effective compared to a 25 mm needle length without digital compression. The single-injection technique for percutaneous peribulbar anesthesia with a short needle is a suitable alternative to

Received 30 August 2013; received in revised form 23 February 2014; accepted 10 March 2014; available online 19 March 2014.

[a] Department of Radiology, King Khaled Eye Specialist Hospital, Riyadh, Saudi Arabia
[b] Mansoura Faculty of Medicine, Diagnostic Radiology Department, Egypt
[c] Department of Anesthesia, St. Michael's Hospital, 30 Bond Street, Toronto, Ontario M5B 1W8, Canada

* Corresponding author at: KKESH, Department of Radiology, P.O. Box 7191, Riyadh 11462, Saudi Arabia. Tel.: +966 502977703.
e-mail address: selkhamary@hotmail.com (S.M. ElKhamary).

☆ Meetings: Abstract presented at 3rd World Congress of ophthalmic anesthesia. May, 2012. Ankara, Turkey.

Peer review under responsibility of Saudi Ophthalmological Society, King Saud University

Production and hosting by Elsevier

Access this article online:
www.saudiophthaljournal.com
www.sciencedirect.com

the double-injection technique for cataract surgery.[5,6] The needle is inserted transcutaneously through the lower eyelid directed into the inferotemporal quadrant with digital pressure applied by the thumb and index fingers around the needle hub during injection.[4,7,8] However the insertion of longer needles increases the potential of injury to important structures. Scott and colleagues demonstrated that a 16 mm needle reaches the vicinity of the orbital equator and cannot pass beyond it.[6]

Magnetic resonance imaging (MRI) with the three-dimensional constructive interference in steady state (3D CISS) sequence is a high resolution, flow compensated gradient echo sequence stimulated to strong T2 weighted image. Additionally, the technique allows multiplanar image reconstruction and therefore excellent anatomical orientation to improve contrast and geometrical resolution.[9–13]

The 3D CISS sequence can be used to investigate a wide range of pathologies when routine MRI sequences do not provide the desired anatomic information. It is frequently used in demonstrating cranial nerves, CSF rhinorrhea and aqueduct stenosis, cisternal spaces, cavernous sinus and the ventricular system.[14–16]

Theoretically, a shorter needle is safer than a longer needle for peribulbar anesthesia and is less likely to damage nerves, vessels, and ocular muscles. However this observation has not been confirmed in human patients. To the best of our knowledge, demonstration of orbital anatomy using a non-invasive diagnostic MRI for anatomical study in relation to ophthalmic anesthesia has not been published in the peer review literature.

The primary aim of this study is to describe the anatomy of the orbital structures with magnetic resonance imaging (MRI) using 3D CISS sequences to provide a morphological basis for the needle entry at 12.5 and 25 mm from the orbital rim. Additionally this study investigates the correlation between the size of the globe and the orbit at the two selected depths.

Methods

A retrospective review was performed on the MRI scans of 50 normal subjects. All the patients referred to the diagnostic imaging department at the King Khalid Eye Specialist Hospital, Riyadh (KKESH) underwent MRI examinations due to different non orbital neurological presentation. This research followed the tenets of the declaration of Helsinki and was approved by the research ethics committee at KKESH (Project Number 102-R with HEC/IRB approval dated 26 March 2011).

Inclusion criteria included, adult patients with non-orbital pathology and normal ocular motility who underwent MRI on a 3-Tesla MR unit using the high resolution 3D CISS sequence. Only images free of motion degradation or other artifacts were selected for analysis. Children, patients with orbital pathology, and those treated with radiation or chemotherapy were excluded from this study as it causes morphological changes that affect the relationship between normal orbital structures. Additionally, patients with myopia, hypermetropia, glaucoma, posterior staphyloma or any other abnormality that could affect the axial length of the globe, were also excluded from the study.

The MRI device used in this study was a Siemens Allegra (Seimen AG, Munich, Germany) operating with 3 T magnet. The orbital MRI examinations were performed with a dedicated head coil. The MRI parameters using the CISS sequence was performed with the following parameters, repetition time (TR) of 10.76 ms, time echo (TE) of 5.38 MS, 70° flip angle, 200 × 200 mm field of view (FOV), 512 × 512 mm matrix, and 64 slices and 0 slice gap. The orbital scan started from the limbus to the orbital apex. Each scan took approximately 6 min including the original 3D CISS sequence and coronal and sagittal MPR images.

The MRI data were transferred to a picture archiving and communication system (PACS) in the original digital imaging and communications in medicine (DICOM) format. The principal investigator (SE, with 20 years MRI experience) reviewed the 3D-CISS sequences and compared the anatomical details at 12.5 and 25 mm depth to assess the significant differences between the orbital structures at the two expected needle depths. The sizes of the globe and the orbit were recorded at the two selected depths using multiplanar reconstruction into axial, coronal and sagittal planes. To reduce measurement errors, the scan images were magnified to enhance accuracy. Orbital structures were compared at depths of 12.5 and 25 mm using multi-planar reconstructions in axial, coronal and sagittal planes to assess the significant differences between the two imaging planes and to assess the size of the globe and the orbit at the two depths using multiplanar reconstruction into axial, coronal and sagittal planes.

Structures that were analyzed included, the size of all extraoccular muscles, orbital fat compartment volume, the presence or absence of the neurovascular bundles and the supporting intermuscular septae structures at the two expected needle depths. The study also assessed the relation of the neurovascular bundle accompanying the muscles at all quadrants as well as the ratio between the size of the globe in relation to the orbital size. Particular attention was given to the measurement of the size of superior ophthalmic vein and the presence or absence of optic nerve tortuosity and its proximity to the needle entry track.

The standard plane for measurement of axial length of eye is the axial section of the eye at the level that showed the insertions of the both medial and lateral rectus muscles and the optic nerve. The axial length of the globe is measured between two imaginary horizontal lines drawn along the corneal apex anteriorly and the scleral rim posteriorly at the approximate location of the fovea (Fig. 1). The diameters were recorded in millimeters (mm).

Maximal thickness of the extraocular muscles was calculated for the following: the maximal muscle thickness of the medial rectus (MR); lateral Rectus (LR); inferior rectus (IR); superior rectus (SR) and; superior oblique (SO). To perform these measurements, the thickness of each muscle was measured directly at the coronal plane on the work stations using direct distance measurement. Distances were measured with a line caliper in millimeters .The volume of the whole muscle was calculated by adding total cross-sectional areas from multiple sections covering the whole muscle and multiplying the sum of areas by the slice increment (slice thickness = 0.7 mm).

The levator palpebrae muscle was included in measurements of the thickness and volume of the SR, because it was difficult to separate the two muscles in the MRI images in some cases. The volume of the inferior oblique muscle

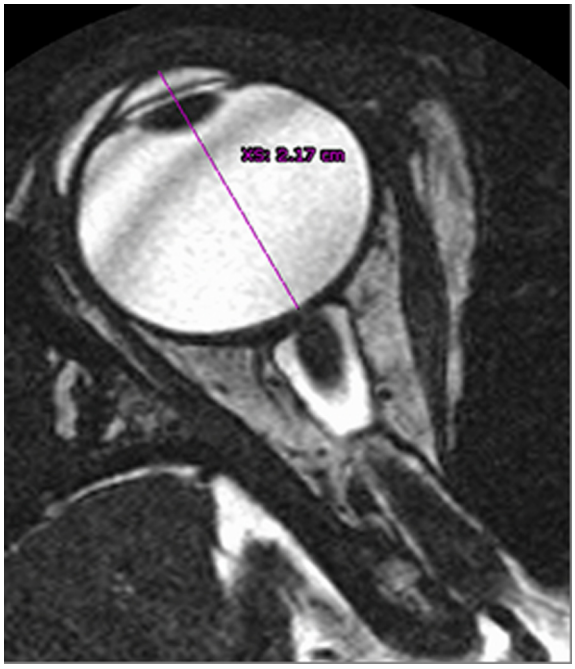

Figure 1. 3D CISS magnetic resonance image axial plan for the right eye showing the standard plane for measurement of the axial length of globe is at the level that shows the insertions of the medial and lateral recti muscles and the optic nerve. The axial length of the globe is measured between two imaginary horizontal lines along the corneal apex anteriorly and the scleral rim posteriorly at the approximate location of the fovea.

was difficult to determine, this was probably because it is very thin at the anterior margin of the orbital floor and its margins are difficult to separate from the surrounding tissues.

The extra-conal fat forms 4 lobes each of which is encapsulated by connective tissue septae. The lobes lie between the insertion of the recti muscles. The volume of each compartment was calculated by adding total cross-sectional areas including the transverse distance between the middle portion of the adjacent ocular wall with the adjacent orbital wall, multiplied by the other longitudinal plane between the tip of the adjacent extraocular muscle, then multiplying the sum of areas by the slice increment (slice thickness = 0.7 mm) (Fig. 2).

The diameter of the superior ophthalmic vein was measured on coronal sections just under the superior rectus muscle at both depths. The measurement was performed on a workstation and the diameters were recorded in mm. Particular attention was given to the superior ophthalmic vein because upper medial quadrant injection was a popular technique, however many authors are against it because of high incidence of periorbital hematoma.

The maximum linear longitudinal and transverse dimension of the bony orbital outline at both depths was performed with electronic calipers available on routine clinical reporting workstations from the coronal images at both depths using the resolution of the original DICOM image. Distances were measured with a line caliper in mm.

Statistical analysis

The results were analyzed using the Statistical Package for Social Science for Windows version 16 (SPSS, Chicago, Ill, USA). Numerical data were expressed as a mean and standard deviation and were analyzed with the unpaired, two-tailed *t*-test. Categorical data were expressed as number

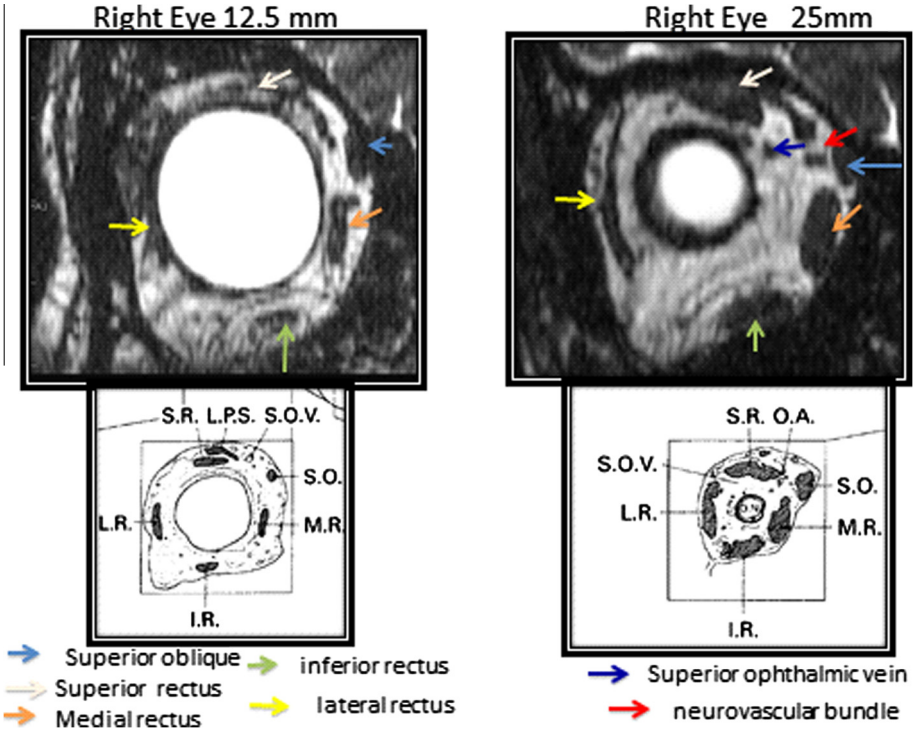

Figure 2. A–D: MRI coronal plan for the right eye, the cross sectional area at 12.5 and 25 mm depths (A,B) and diagram (C,D) at same plan showed maximal thickness of extraocular muscle with the relatively large volume of fat containing space. More posteriorly, the structures are packed together and the inferior and lateral rectus muscle bellies become larger and closer with little intervening fat close to the orbital floor. More posteriorly, the posterior orbital fat is smaller in comparison to the size of the muscle belly.

Table 1. Measurement of extraocular muscles and fat areas at 12.5 and 25 mm levels.

	12.5 mm cut (n = 50)	25 mm cut (n = 50)	P value
Lateral rectus muscle (cm^3)	0.26 (0.07)	0.33 (0.06)	0.001
Inferior rectus muscle (cm^3)	0.26 (0.06)	0.37 (0.03)	0.001
Medial rectus muscle (cm^3)	0.27 (0.05)	0.38 (0.04)	0.001
Superior rectus muscle (cm^3)	0.16 (0.06)	0.28 (0.04)	0.001
External oblique aponeurosis (cm^3)	0.13 (0.05)	0.25 (0.05)	0.001
Inferior temporal fat (cm^3)	1.38 (0.61)	1.10 (0.68)	0.033
Inferior nasal fat (cm^3)	1.13 (0.51)	1.23 (0.62)	0.34
Superior nasal fat (cm^3)	0.43 (0.26)	0.48 (0.33)	0.35

Table 2. Measurement of different orbital and vascular structures at 12.5 and 25 mm levels.

	12.5 mm cut (n = 50)	25 mm cut (n = 50)	P value
Size of the globe (cm)	1.82 (0.27)	2.41 (0.14)	0.001
Size of the orbit (cm)	3.49 (0.48)	3.99 (0.18)	0.001
Inferior temporal NVB			
Present	20	31	0.91
Absent	30	19	
Inferior nasal NVB			
Present	19	25	0.67
Absent	31	25	
Superior nasal NVB			
Present	34	39	0.51
Absent	16	11	
Superior temporal NVB			
Present	19	34	0.39
Absent	31	16	
Septa between LR & IR			
Present	9	14	0.318
Absent	41	36	
Septa between MR & IR			
Present	8	8	0.53
Absent	42	42	
Septa between levator SR & LR			
Present	29	24	0.77
Absent	21	26	

and percentages and compared using χ^2 test. $P \leqslant 0.05$ was considered statistically significant.

Results

The study sample was comprised of 50 patients (30 (60%) females, 20 (40%) males). The mean age was 52.3 years. We examined 26 (52%) right eyes and 24 (48%) left eyes.

Table 1 presents the measurement of extraocular muscles and fat at 12.5 and 25 mm, The cross sectional area of the extraocular muscles was statistically significantly smaller at the 12.5 mm plane ($P = 0.001$). The inferotemporal fat area was statistically significantly larger at the 12.5 mm plane ($P = 0.033$). There was no difference in the inferonasal areas between the two depths ($P = 0.34$). There was no difference in the superonasal fat areas between the two depths ($P = 0.35$).

The measurements of the different orbital and vascular structures at 12.5 and 25 mm depths are presented in Table 2. The size of the orbit and globe was statistically significantly larger at 12.5 mm ($P = 0.001$). There was no difference between depths in the presence or absence of the neurovascular bundles and the supporting structures including the intramuscular septae.

Discussion

The outcomes of this study indicate that the 3D CISS MRI scanning demonstrated that there is a larger structure free space at orbital depths of 12.5 than 25 mm which was useful as a non-invasive sequence to confirm the presumed clinical findings that there was greater free space for the important orbital structures at 12.5 mm compared to the 25 mm depth. 3D CISS MRI with multi-planar reconstructions in axial, coronal and sagittal planes provides an excellent method to demonstrate the orbital anatomy in relation to ophthalmic anesthesia and to characterize the relationship between the adjacent orbital structures with high spatial intrinsic resolution.

The orbit can be divided into 3 anatomical spaces (anterior, mid and posterior) for a better appreciation of the relationship of the injection site.[18] The mid-orbit ends posteriorly about 10–12 mm from the back surface of the globe. It contains primarily muscle bellies and adipose connective tissue. The posterior orbit ends at the optic canal and consists mainly of muscle origins and a collection of neurovascular bundles.[18,19]

From this classification, it is clear that a longer needle will have the potential to cause injury to important orbital structures. In particular, patients with shallow orbits with tortuous optic nerves are at a greater risk.

A previous study of 150 patients reported that a 15 mm needle with digital pressure (with thumb and index finger around the needle hub during injection) gives comparable results to a 25 mm needle.[17]

Liu et al.[20] investigated the MRI appearance of the optic nerve in extremes of gaze with implications for the position of the globe for retrobulbar anesthesia and showed that the safe locations for needle insertion are at the extreme inferotemporal corner of the orbit and in the medial area due to a compartment with larger volumes of fat containing adipose connective tissue. Our results using the CISS sequence concur with Liu et al.[20] For example, we found that the inferotemporal fat area is statistically significantly larger at the 12.5 mm plane ($P = 0.033$). At deeper planes, the structures are more tightly packed together and the posterior orbital fat is smaller in comparison to the size of the inferior and lateral recti muscle bellies which are closer to each other with little intervening fat at the orbital floor and lateral orbital wall respectively.

Conclusion

There is a larger structure-free space at a depth of 12.5 than at 25 mm. Therefore, the inference is that, a needle inserted in the infero-temporal zone to a depth of 12.5 mm is

less likely to injure the eyeball or extra-ocular muscles than one advanced to 25 mm.

Conflict of interest

The authors declared that there is no conflict of interest.

Reference

1. Riad W, Nauman A. Single injection peribulbar anesthesia with a short needle combined with digital compression. *Anesth Analg* 2008;**107**:1751–3.
2. Winder S, Walker SB, Atta HR. Ultrasonic localization of anesthetic fluid in sub-Tenon's, peribulbar, and retrobulbar techniques. *J Cataract Refract Surg* 1999;**25**:56–910.
3. Ripart J, Metge L, Prat-Pradal D, Lopez FM, et al. Medial canthus single injection episcleral (sub-tenon anesthesia): computed tomography imaging. *Anesth Analg* 1998;**87**:42–5.
4. Van den bergs AA. An audit of peribulbar blockade using 15 mm, 25 mm and 37.5 mm needles and sub-Tenon's injection. *Anaesthesia* 2004;**59**:775–80.
5. Mahdy RA, Ghanem MT. Comparison between single-injection inferomedial and inferotemporal peribulbar blockades before cataract surgery. *Ophthalmologica* 2012;**227**:111–4.
6. Scott R, Jakeman C, Perry S, Acharya P. Peribulbar anaesthesia and needle length. *J R Soc Med* 1995;**88**:594–6.
7. Sun X, Liang C, Liu C, Liu S, Deng K, He J. Oculomotor paralysis: 3D-CISS MR imaging with MPR in the evaluation of neuralgic manifestation and the adjacent structures. *Eur J Radiol* 2010;**73**(2):221–3 Feb.
8. Ghali AM, Mahfouz AK, Hafez A. Single-injection percutaneous peribulbar anesthesia with a short needle versus sub-Tenon's anesthesia for cataract extraction. *Saudi J Anaesth* 2011;**5**:138–41.
9. Chavhan GB, Babyn PS, Jankharia BG, Cheng HL, Shroff MM. Steady-state MR imaging sequences: physics, classification, and clinical applications. *Radiographics* 2008;**28**:1147–60.
10. Casselman JW, Kuhweide R, Deimling M, et al. Constructive interference in steady state-3DFT MR imaging of the inner ear and cerebellopontine angle. *AJNR Am J Neuroradiol* 1993;**14**:47–57.
11. Castillo M. Imaging of the upper cranial nerves I, III–VIII, and the cavernous sinuses. *Magn Reson Imaging Clin N Am* 2002;**10**:415–31.
12. Held P, Fellner C, Fellner F, Seitz J, Strutz J. MRI of inner ear anatomy using 3D MP-RAGE and 3D CISS sequences. *Br J Radiol* 1997;**70**:465–72.
13. Yousry I, Camelio S, Schmid UD, et al. Visualization of cranial nerves I–XII: value of 3D CISS and T2-weighted FSE sequences. *Eur Radiol* 2000;**10**:1061–7.
14. Roser F, Ebner FH, Danz S, Riether F, Ritz R, Dietz K, et al. Three-dimensional constructive interference in steady-state magnetic resonance imaging in syringomyelia: advantages over conventional imaging. *J Neurosurg Spine* 2008;**8**:429–35.
15. Ramli N, Cooper A, Jaspal T. High resolution CISS imaging of the spine. *Br J Radiol* 2001;**74**:862–73.
16. Thomas B, Krishnamoorthy T, Aravinda HR, Kesavadas C. 3D-CISS MRI in a purely intracanalicular cochlear schwannoma. *J Neuroradiol* 2008;**35**:305–7.
17. Riad W. Administration of extraconal anesthesia: what care providers should know? *Radiol Saudi J Anaesth* 2007;**1**(1):1–2.
18. Unsöld R, Stanely JA, et al. The CT topography of retrobulbar anesthesia: anatomic-clinical correlation of complications and suggestions of a modified technique. *Graefes Arch Clin Exp Ophthalmol* 1981;**217**:125–36.
19. Ettl A, Salomonowitz E, Koornneef L, Zonneveld FW. High-resolution MR imaging anatomy of the orbit. *Clin North Am* 1998;**36**:1021–45.
20. Liu C, Youl B, Moseley I. Magnetic resonance imaging of the optic nerve in extremes of gaze. Implications for positioning of the globe for retrobulbar anaesthesia. *Br J Ophthalmol* 1992;**76**:728–33.